M. J. Levine, and A. Z. Schwarzschild, Phys. Lett. 47B, 231 (1973).
[3]C. Chasman, S. Kahana, and M. J. Schneider, Phys. Rev. Lett. 31, 1074 (1973).
[4]W. E. Frahn and R. H. Venter, Ann. Phys. (New York) 24, 243 (1963).
[5]V. M. Strutinskii, Zh. Eksp. Teor. Fiz. 46, 2078 (1964) [Sov. Phys. JETP 19, 1401 (1964)].
[6]A. Dar, Nucl. Phys. 55, 305 (1964), and Phys. Rev. 139, B1193 (1965), and Nucl. Phys. 82, 354 (1966).
[7]J. V. Maher, K. E. Erb, G. H. Wedberg, J. L. Ricci, and R. W. Miller, Phys. Rev. Lett. 29, 292 (1972).
[8]P. R. Christensen, O. Hansen, J. S. Larsen, D. Sinclair, and F. Videbaek, Phys. Lett. 45B, 107 (1973).
[9]P. Braun-Munzinger, W. Bohne, C. K. Gelbke, W. Grochulski, H. L. Harney, and H. Oeschler, Phys. Rev. Lett. 31, 1423 (1973).
[10]A. Cunsolo, M. C. Lemaire, M. C. Mermaz, and H. Sztark, to be published; M. C. Mermaz, unpublished.
[11]G. C. Morrison, J. Phys. (Paris), Colloq. 33, C5-111 (1972).
[12]B. Zeidman, W. Henning, and D. G. Kovar, to be published.
[13]R. M. DeVries, Phys. Rev. C 8, 951 (1973).
[14]N. Austern and J. S. Blair, Ann. Phys. (New York) 33, 15 (1965).
[15]W. E. Frahn and M. A. Sharaf, Nucl. Phys. A133, 593 (1969).
[16]J. S. Blair, Phys. Rev. 115, 928 (1959).

# Self-Consistent Solution for an Axisymmetric Pulsar Model

L. G. Kuo-Petravic
*Atlas Computer Laboratory, Chilton, Didcot, Berkshire, England, and St. Hilda's College, Oxford, England*

and

M. Petravic
*Department of Engineering Science, Oxford, England*

and

K. V. Roberts
*Culham Laboratory, Abingdon, Berkshire, England*

(Received 19 February 1974)

A spinning neutron star surrounded by a magnetosphere is widely accepted as the basic pulsar model. We have obtained a self-consistent numerical solution for the case when the rotation and magnetic axes are aligned. The field lines close even beyond the light radius $R_L$, and with Crab-pulsar parameters $5\times10^{37}$ erg/sec are carried away by relativistic particles. An equatorial region of high-energy density is found near $R_L$ which could be the region of observed radio emission.

The assumption of a conducting neutron star[1-3] and an imbedded magnetic field fixes the star boundary conditions for the electromagnetic field. There is more freedom in the choice of the equations describing the particle motion in the magnetosphere[4] and the appropriate physical boundary conditions. We have chosen relativistic fluid equations to describe the average particle motion, and they together with Maxwell's equations form the following closed set whose self-consistent solution should describe the behavior of the magnetosphere:

$$\partial n_\pm/\partial t = -\nabla\cdot(n\vec{v})_\pm + \eta\nabla^2 n_\pm, \quad \partial(mn\vec{v})_\pm/\partial t = -\nabla\cdot(mn\vec{v}\vec{v})_\pm \pm en_\pm(\vec{E}+c^{-1}\vec{v}_\pm\times\vec{B}) + \eta\nabla^2(mn\vec{v})_\pm,$$
$$-c^{-1}\partial\vec{B}/\partial t = -\nabla\times\vec{E}, \quad c^{-1}\partial\vec{E}/\partial t = \nabla\times\vec{B} - 4\pi e[n_+\vec{v}_+ - n_-\vec{v}_- - \eta\nabla(n_+ - n_-)]/c. \tag{1}$$

The subscripts $\pm$ refer to the positively and negatively charged particles, $n$ and $\vec{v}$ are particle density and velocity, and the relativistic mass is $m = m_0\gamma$. The same absolute charge $e = 4.8\times10^{-10}$ esu has been assumed for both particle species. The artificial diffusion term $\eta\nabla^2 n$ in the continuity equation and the corresponding terms in the other equations are small ($\eta\approx10^{-3}R_L{}^2\Omega$, where $R_L = c/\Omega$ is the light-cylinder radius, $c$ the speed of light, and $\Omega$ the angular velocity) and have been introduced to improve numerical stability. The pressure term has been omitted from the momentum equation because it is either small

compared to the Lorentz-force term or small compared to the inertial terms.

For the inner boundary conditions it is assumed that, depending on the sign of the normal component of the electric field, either positively or negatively charged particles are emitted, with a velocity proportional to $\vec{b}(\vec{E}\cdot\vec{b})$, where $\vec{E}$ is the electric field and $\vec{b}$ the unit vector in the direction of the magnetic field $\vec{B}$. Any particles striking the inner boundary are absorbed. Vacuum conditions are assumed to apply to $\vec{B}$ on the outer boundary at $R_1 = 4R_L$, and the radial velocity condition $v_r^{\pm}(R_1) \geq 0$ is required of both species of particle. For convenience the inner boundary is taken at $R_0 = 0.2R_L$; and, provided the magnetosphere there is a good conductor, the same boundary conditions can be used for the fields as if the boundary were on the star surface. The particle density on the inner boundary is taken close to the values corresponding to the solution of an equivalent perfect-conductor problem, i.e.,

$$n \approx (4\pi ec)^{-1}\nabla\cdot[\vec{r}\times\vec{\Omega})\times\vec{B}]$$

at $r = R_0$. In order to allow for possible unsteady flows, the initial conditions assume the star at rest in a vacuum surrounded by a dipole magnetic field. The star is then put into rotation around the dipole axis, its angular frequency increasing linearly with time until a final value is reached:

$$\omega(t) = \Omega t/T \text{ for } 0 \leq t \leq T,$$
$$= \Omega \text{ for } t > T.$$

This is reflected in the boundary conditions for the electromagnetic fields on the inner boundary, which in spherical polar coordinates become

$$B_r(R_0) = B_L(R_L/R_0)^3 2\cos\theta, \quad E_\varphi(R_0) = 0,$$
$$E_\theta(R_0) = -\omega(t)B_r(R_0)R_0\sin\theta,$$

where $B_L = B_\theta(R_L)$. Equations (1) have been solved numerically as a function of time using a spherical polar mesh of typically $20\times200$ mesh points and a leap-frog explicit finite-difference scheme. The time step $\Delta t$ was such that $600\Delta t = \tau$ and $800\Delta t = T$, where $\tau$ is the final steady period of rotation $\tau = 2\pi/\Omega$. Typically, the region of computation was $0 \leq \theta \leq \pi/2$ and $0.2R_L \leq r \leq 4R_L$. Assuming values of $B_L$ of up to $10^6$ G, the equations could not be solved numerically for the actual electron and ion rest masses. The rest masses $m_0$ for both particle species were therefore given increased and equal values for the purposes of the calculation, but subject to the condition that the inertial terms were, on average, not more than 5% of either of the two almost-canceling terms in the Lorentz force in regions where the relativistic factor $\gamma = [1-(v/c)^2]^{-1/2} \leq 2$. Specifically, we make $m_0$ a function of space according to $m_0 = (\alpha/\Omega)eB_\theta/c$ with $\alpha = \Omega(eB_\theta/m_0c)^{-1} = 0.05$. The effect of this choice can be illustrated by the error it produces in the radial component of the electric field on the equator. In a steady state,

$$m_0\gamma v_\varphi^2/er + E_r + v_\varphi B_\theta/c = 0.$$

Inserting the expression for $m_0$ we find $E_r = (r\Omega B_\theta/c)(1-\alpha\gamma)$. Similar estimates can be made in other regions of space and one finds that the difference between values given by our equations and those obtained by solving $\vec{E}+\vec{v}\times\vec{B}/c = 0$ is around 5% for $\gamma \approx 1$. The latter equation, however, is not valid beyond $r = R_L$, while the accuracy of our equations improves with increasing $\gamma$, the least-accurate region being that where $2 \leq \gamma \leq 5$. Since the results indicate particle energies up to $10^{16}$ eV, the errors introduced by our "large" mass are small compared to assuming negligible inertial terms beyond $R_L$. In this way the model has become independent of $R_L$ and $B_L$, provided $B_L$ is not too low.

The pattern of flow reached at one rotation period past the end of acceleration ($t = T + \tau$) is shown in Fig. 1. While the "polar" particles [negatively (positively) charged if the angular frequency vector is parallel (antiparallel) to the magnetic moment] are seen to follow the "field lines" $\vec{B}_{r\theta} = \vec{a}_r B_r + \vec{a}_\theta B_\theta$, the "equatorial" particles cross them beyond $R_L$ and to a smaller extent for $r < R_L$. This seems unavoidable since the last field line which closes within $R_L$ and delimits the corotating "quiet zone"[4,5] connects to the inner boundary in the negatively charged region as can be seen by comparing Fig. 2 with Fig. 3. Note that the dividing neutral line is 10° closer to the equator than the $\theta \approx 55°$ line which would obtain for a perfect conductor, while the charge densities are fractionally lower than the perfect-conductor values. It is also found that the radial velocity on the equator increases from virtually 0 at $0.8R_L$ to $0.5c$ at $1.2R_L$, while the azimuthal velocity $v_\varphi$ is greater than $r\Omega$ up to $r = 0.95R_L$ where it reaches the maximum of $0.95c$. In contrast, the "polar" particles are being accelerated more gradually, $v_r$ increasing approximately as $v_r = 0.5cr/R_L$ which incidentally results in $n(\theta=0) \sim 1/r^3$, as in the perfect conductor case, except that the falloff is sharper for small $r$, and as a consequence the densities beyond $r = 0.5R_L$ are down by a factor of 4 on the perfect-conductor

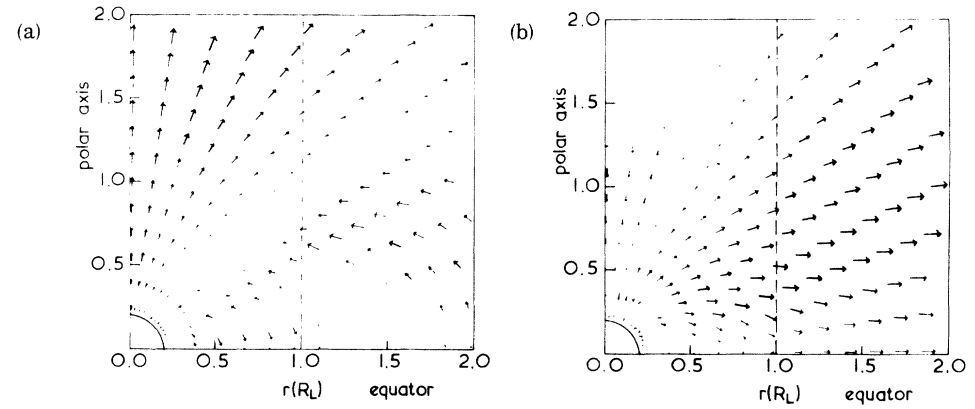


FIG. 1. Flow patterns for (a) "polar" and (b) "equatorial" particles at time $t = T + \tau$ presented as projections of the respective velocity fields onto the $r$-$\theta$ plane. The arrows are given by $\vec{v}_{r\theta} = (0.125/c)(\vec{a}_r v_r + \vec{a}_\theta v_\theta)$, and the empty regions signify zero densities. Here $\vec{a}_r$ and $\vec{a}_\theta$ are coordinate-system unit vectors.

values.

We find that the flow patterns are almost steady in the polar and equatorial regions and that the fluctuations in the total particle fluxes between $R_L$ and $3R_L$ are less than 15%. There are, however, oscillations around zero radial motion in the equatorial "quiet zone" and the region close to the neutral (zero charge) line appears to be unsteady. It is not yet possible to say whether this is a permanent feature, but the fact that the magnetic field lines cross the neutral line at a rather large angle may require flows across the field lines, which implies a nonzero $E_\varphi$ and the lack of a steady solution. While the existence or nonexistence of a truly steady state remains to be proved, the mean values around which oscillations occur have been established. The flows beyond $R_L$ appear particularly steady, thus enabling us to determine particle and energy fluxes. We find that with $\Omega = 200$ and $B_L = 10^6$ G (Crab-pulsar parameters, apart from uncertainty in $B_L$) that a total of $2\times10^{33}$ particles/sec cross the outer boundary, and the energy loss is $5\times10^{37}$ erg/sec. The magnetic field is twisted in the $\varphi$ direction in accordance with the corresponding torque. The maximum energy of the equatorial particles

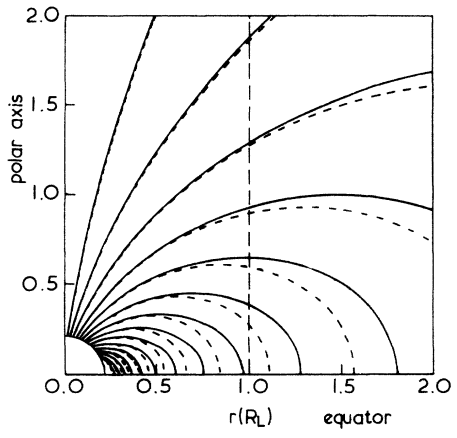


FIG. 2. Field lines of $\vec{B}_{r\theta} = \vec{a}_r B_r + \vec{a}_\theta B_\theta$ at $t = T + \tau$. These are shown rather than the projection of the field lines of $\vec{B}$ in order to facilitate comparison with Fig. 1, since the origins of the projected velocity vectors all lie in a $\varphi$ = const plane. Dashed lines, static magnetic dipole field lines corresponding to the magnetic induction field $\vec{B}$ at $t = 0$.

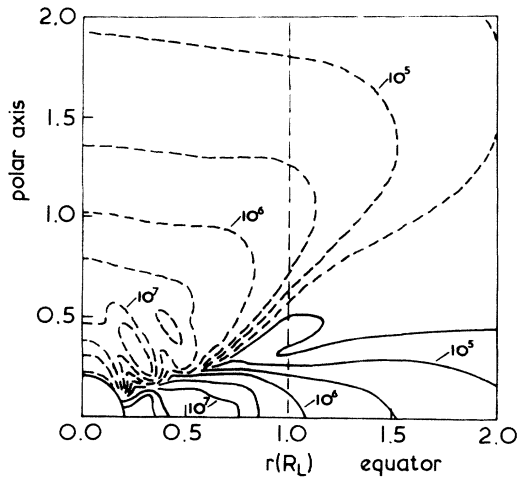


FIG. 3. Contours of charge densities in the $r$-$\theta$ plane. Solid and dashed lines refer to the signs of charge corresponding to the "equatorial" and "polar" species, respectively. The numbers beside the contours are in particles/cm$^3$.

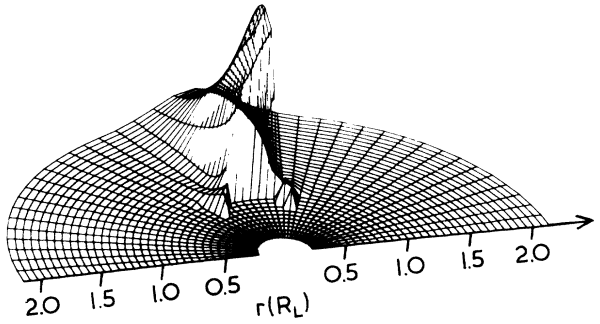


FIG. 4. The energy density surface as a function of the polar coordinates in the range $0.2R_L \leq r \leq 2.2R_L$ and $0 \leq \theta \leq \pi$. The maximum is at $r = 0.9R_L$ and $\theta = \pi/2$ and corresponds to $2.8 \times 10^{10}$ erg/cm$^3$.

is about twice their average energy which equals $3 \times 10^{16}$ eV. As $\frac{2}{3}$ of this energy is gained beyond $R_L$, and since $E_r(r, \theta = \frac{1}{2}\pi)$ for $r > R_L$ depends little on particle mass, we estimate that our average energy is on the large side by less than a factor of 2. (If the true particle masses had been used, less energy might have been gained in the $r < R_L$ region because of better screening and a smaller centrifugal term.) The "polar" particles gain energy much more slowly and the energy flux carried by them is down by more than 2 orders of magnitude. There are reasons to believe that the ratio of the energy fluxes for the "equatorial" and "polar" particles will remain high all the way to "infinity" or the nebula. Since the main acceleration mechanism is the radial component of the electric field under conditions $E_r + mv_\varphi^2/r > B_\theta$, the highest energies and energy densities are found, not unexpectedly, on the equator in the region $R_L < r < 2R_L$. A view of the energy-density surface is shown in Fig. 4.

What are the implications of these results for the assumption that pulsars are magnetic neutron stars? If it were not for the uncertainty in the assumed magnetic field strength ($10^6$ G on the light radius or $\sim 8 \times 10^{12}$ G on the star surface, about the same as required for the vacuum rotator models[6-9]), one could say that the results confirm the hypothesis. Apart from providing $5 \times 10^{37}$ erg/sec to the Crab nebula as required by the observations, what gives conviction to the model is the fact that the energy is very unequally distributed among particles of different charge, and on observational evidence one would conclude that the equatorial particles are electrons. Finally, energy density is concentrated in a thin ring of radius $R_L$, which is a simple consequence of the fact that the magnetic field lines do not open at or near the light radius, the most conclusive and important result of our computation. The potential drop along the polar axis is found to be relatively small at least up to the outer boundary of the present calculation. There is evidence that these results do not depend significantly on the initial conditions, but this point merits a more thorough examination. While it is not entirely safe to extrapolate all of the features of our parallel-rotator model to an oblique one, taking into account the known vacuum-field configuration[9,10] of the latter it seems plausible that the ring would degenerate into two regions of high-energy density.

We are very grateful to the Science Research Council and its Atlas Computer Laboratory for making available excellent computing facilities.

[1]T. Gold, Nature (London) 218, 731 (1968).
[2]G. Baym, C. J. Pethick, and D. Pines, Nature (London) 223, 674 (1969).
[3]M. Ruderman, Annu. Rev. Astron. Astrophys. 10, 427 (1972).
[4]P. Goldreich and W. H. Julian, Astrophys. J. 157, 869 (1969).
[5]L. Mestel, Nature (London) 233, 149 (1971).
[6]F. Pacini, Nature (London) 219, 145 (1968).
[7]J. P. Ostriker and J. E. Gunn, Astrophys. J. 157, 1395 (1969).
[8]J. E. Gunn and J. P. Ostriker, Phys. Rev. Lett. 22, 728 (1969).
[9]V. G. Endean and J. E. Allen, Nature (London) 228, 348 (1970).
[10]A. J. Deutsch, Ann. Astrophys. 18, 1 (1955).